

High-Definition Field Texture Measurements for Predicting Pavement Friction

Natalia Zuniga-Garcia, M.Sc.

Graduate Research Assistant

nzuniga@utexas.edu

Department of Civil, Architectural and Environmental Engineering

The University of Texas at Austin

ECJ Bldg., Ste. 6.506 (C1761), Austin, TX 78712

Jorge A. Prozzi, Ph.D.

Professor

prozzi@mail.utexas.edu

Department of Civil, Architectural and Environmental Engineering

The University of Texas at Austin

ECJ Bldg., Ste. 6.10 (C1761), Austin, TX 78712

The following paper is a pre-print, the final publication can be found in Transportation Research Record, No. 2673: 246–260, 2019.

Zuniga-Garcia, N., & Prozzi, J. A. (2019). High-Definition Field Texture Measurements for Predicting Pavement Friction. *Transportation Research Record*, 2673(1), 246–260. <https://doi.org/10.1177/0361198118821598>

ABSTRACT

Monitoring and managing skid resistance properties are crucial activities to reduce the number of highway accidents and fatalities. However, current methodologies to measure pavement surface friction present several disadvantages that make them impractical. Thus, it is necessary to evaluate alternative methods to estimate friction. The principal objective of this study was to develop friction models based on pavement texture. We implemented a Line Laser Scanner (LLS) to obtain an improved characterization of the pavement texture which includes macrotexture and incorporates microtexture description using eight different parameters. Field measurements of friction and texture were collected around Texas using the British Pendulum Test (BPT), the Dynamic Friction Test (DFT), the micro-GripTester, and the LLS. The experimental results showed that there is not a unique relationship between texture and friction, its relation is strong and statistically significant, but it is different for each type of pavement surface. Thus, regression analysis pooling all data cannot be utilized to quantify this relationship. For this reason, we applied a panel data analysis approach that allows the incorporation of the type of surface and provides a more robust analysis. The results indicate that the prediction of friction is significantly improved when incorporating information from both macrotexture and microtexture into the prediction model. Therefore, a measure of microtexture should be included into friction models based on texture. Also, the study of different texture parameters suggests that the mean profile depth (MPD) is the most significant parameter for macrotexture and for microtexture to explain the distinct friction measures.

1 *Keywords:* friction, skid resistance, macrotexture, microtexture, laser scanner, data analysis.

2 INTRODUCTION

3 Highway surface skid resistance has a significant influence on the number of wet weather
4 accidents. Research conducted by the National Transportation Safety Board (NTSB) and the
5 Federal Highway Administration (FHWA) in 1980 indicates that about 70% of wet pavement
6 crashes can be prevented or minimized by improving pavement friction (1). Therefore, monitoring
7 and managing skid resistance properties is crucial to reduce the number of highway accidents and
8 fatalities. Pavement surfaces should be designed, constructed, and maintained to provide durable
9 and adequate skid resistance properties for drivers. Current methodologies to measure pavement
10 surface friction present several disadvantages that make them impractical for field data collection
11 over large highway networks. For instance, most tests require water application to simulate the
12 wet condition. The use of water limits the continuity of the test over long distances and affects its
13 efficiency. Additionally, some methods require traffic control, which can be costly, time-
14 consuming and present safety concerns. Thus, it is important to study different ways to estimate
15 surface friction characteristics based on other properties that are easier to measure at a network
16 level.

17 It is widely recognized that surface texture is the primary pavement property controlling
18 skid resistance (2). Highway texture is classified into three main categories based on a range of
19 wavelengths and amplitudes (3). The first category, microtexture (wavelengths lower than 0.5
20 mm), refers to the small-scale texture of the aggregate surface. The second category is the
21 macrotexture (wavelengths of 0.5 to 50 mm), which refers to the large-scale texture of the
22 pavement surface due to the aggregate particle size and arrangement. The third category,
23 megatexture, has wavelengths in the same order of size as the tire-pavement interface (50 to 500
24 mm). The microtexture and the macrotexture are the two key pavement surface characteristics
25 necessary for the development of good skid resistance. It is commonly accepted that microtexture
26 controls the wet and dry friction at low speeds, while the macrotexture controls the friction at high
27 speeds (4).

28 A conventional approach to describe the influence of pavement texture on surface friction
29 is using empirical modeling (4). However, due to the limitations for measuring small wavelengths,
30 many of the texture and friction relations have been implemented using only macrotexture (5, 6,
31 7) or a surrogate measure of microtexture (8). Thus, the individual effects of each texture
32 component have not been quantified, and their contribution to skid under different conditions of
33 moisture, speed, and highway conditions are not well understood. The research on the effect of
34 incorporating both texture component into the friction models is limited.

35 Recent developments in optics and computers allowed the collection of high definition
36 images of the surface of the highway pavement. Some researchers have attempted to incorporate
37 microtexture to the skid resistance prediction using non-contact technologies to characterize
38 microtexture. For example, Li et al. (9), Serigos et al. (10), and Alhasan et al. (11) used laser
39 scanners to obtain a surface profile that included microtexture wavelengths. However, the main
40 challenge remains in the surface characterization. Currently, there are no standardized methods for
41 microtexture characterization, and some macrotexture parameters are too simplistic and do not
42 describe the distribution of the profile, which is critical for assessing friction characteristics.

43 The principal objective of this research is to investigate the effect of different texture
44 components and their parametric description on the skid resistance of a pavement surface. We
45 implemented a Line Laser Scanner (LLS) to make an improved characterization of the road texture,

1 including macrotexture and microtexture descriptions, and we used signal processing techniques
2 to separate the effect of the different texture components. The methodology consists of field
3 measurements of friction and texture on different surfaces on the Texas highway network using
4 various technologies. The friction characterization tests include the British Pendulum test (BPT),
5 the Dynamic Friction test (DFT), and the micro-GripTester. Furthermore, we evaluated and
6 compared distinct surface texture parameters to determine the better predictors of friction.

7 The main contributions of the present paper are: (1) the evaluation of the effect of
8 predicting skid resistance using both macrotexture and microtexture components obtained from
9 field data collection; (2) the comparison of friction measures obtained using different test methods
10 (BPT, DFT, and micro-GripTester); (3) the quantification of different macrotexture and
11 microtexture parameters to determine the better predictor of friction; and (4) the evaluation of
12 texture and friction characteristic of different surface types.

13 The subsequent sections of this paper are organized as follows. The “Background” section
14 provides a description of the friction and texture concepts and measuring methods. “Methodology”
15 describes the implementation of the LLS and the field data collection process. The “Statistical
16 Analysis” section describes the data analysis technique, the models evaluated, and the statistical
17 analysis we performed. “Results and Discussion” presents the main results and a discussion of the
18 results. The final section, “Summary and Conclusions,” summarizes the main findings.

19 **BACKGROUND**

20 This section provides definitions for friction and texture, as well as the description of most
21 common methods used to measure and test these surface properties.

22 **Friction and Skid Resistance**

23 Pavement friction is the force that resists the relative motion between a vehicle tire and the
24 pavement surface (4). Skid resistance is the ability of the traveled surface to prevent the loss of tire
25 traction (12). The skid resistance is commonly quantified by the coefficient of friction multiplied
26 by 100 and reported as skid number (SN). There are two types of friction that are usually measured:
27 the side forced friction and the longitudinal friction. Several different friction-measuring devices
28 have been developed based on the main principle of a rubber element sliding over the road surface
29 and measuring the reaction force. The three major operating principles of frictional measurement
30 equipment are (13): slider, longitudinal friction coefficient (LFC), and side force coefficient (SFC).
31 It should be noted that friction is not a unique value as it depends on many different variables that
32 affect the interaction between the tire and the pavement surface.

33 The slider principle covers devices used for stationary testing; therefore, they are mainly
34 used in the laboratory or require traffic control. The most commonly used devices worldwide are
35 the British Pendulum Test (BPT) and the Dynamic Friction Test (DFT). The BPT is manually
36 operated and provides a spot measurement of the surface friction. It measures the friction
37 coefficient at a skidding speed of approximately 10 km/h (14). Therefore, it evaluates the skid
38 resistance at low speed. The DFT is a modular system that is controlled electronically to measure
39 friction by the rotating principle. It measures the torque necessary to rotate three rubber sliders in
40 a circular path at different speeds. Results are typically recorded at a range of speeds from 10 to
41 80 km/h, and the speed versus friction relationship can be obtained (12).

42 Pulled devices methods utilize one or two test tires to measure pavement friction properties
43 using the LFC or SFC principles. The locked-wheel test is the most commonly used method for
44 measure longitudinal pavement friction at high-speed in the United States (4, 14). This method is
45 meant to test the frictional properties of the surface under emergency braking conditions for a

1 vehicle without anti-lock braking system (ABS). The fixed-slip techniques measure friction
2 experienced by cars with ABS. Examples of the fixed-slip tester are the GripTester and the micro-
3 GripTester. They can measure continuously and dynamically the longitudinal skid resistance
4 coefficient of the pavement, expressed as Grip Number (GN). They have a single measuring wheel,
5 fitted with a particular smooth tread tire that is mounted on an axle instrumented to measure both
6 the horizontal drag force and the vertical load force (15). The GripTester is towed behind a vehicle,
7 and its measuring speed ranges from 5 to 100 km/h. The micro-GripTester is performed manually
8 at a recommended walking speed of 2.5 km/h.

9 **Texture**

10 Pavement texture is the most important feature of the pavement surface that ultimately determines
11 most tire-pavement interactions, including friction, noise, splash-and-spray, rolling resistance, and
12 tire wear (14). Different equipment and techniques are used to quantify texture depending on the
13 component being measured.

14 *Measuring Texture of Pavement Surfaces*

15 The macrotexture is commonly described by indirect measures using volumetric techniques, such
16 as the Sand Patch, the Grease Patch or the Outflow Meter. The Sand Patch test is known as the
17 classical macrotexture measure technique. The method requires the use of solid glass spheres or
18 Ottawa natural silica sand. The sand is spread on a pavement in a circular motion with a spreading
19 tool. The known volume of sand divided by the area of the circle is reported as the Mean Texture
20 Depth (MTD), resulting in a measurement representing an area.

21 Advances in technology allow the direct measure of the texture profiles using non-contact
22 lasers, such as the Circular Track Meter (CTM) and the Laser Texture Scanner (LTS). The
23 information collected can be used to compute various profile statistics, for example, the Mean
24 Profile Depth (MPD). The MPD is a line measurement that is estimated by splitting the texture
25 profile into segments of 100 mm in length. The segment is divided into two halves, and the height
26 of the highest peak within each half is determined. The average of these two peaks is referred to
27 as the mean segment depth. The average value of the mean segment depth of the measured profiles
28 is the MPD. Therefore, while MPD is a one-dimensional measurement (linear property), MTD is
29 a two-dimensional measurement (surface property).

30 Currently, there are no standard methods to measure microtexture. Research on the
31 measurement of microtexture is mainly based on the use of laser scanners (9, 10, 11) or image
32 analysis technique such as the Aggregate Imaging System (AIMS) (16). Although, due to issues
33 with field measurement of microtexture and its high correlation with low-speed friction, low-speed
34 friction test measures are commonly used as a surrogate for quantifying microtexture (8).

35 *Texture Characterization*

36 The characterization of texture consists of the use of summary statistics usually referred to as
37 parameters. For macrotexture characterization, there are several well-defined and widely used
38 parameters; the most common are the MPD and MTD. In the pavement engineering literature,
39 there are no standardized methods for microtexture characterization; however, different parameters
40 are described to characterize microtexture, including those used to describe macrotexture. The
41 development of new equipment for digitizing surfaces allows the implementation of a series of
42 experimental characterization procedures. Recent evaluations have focused on the study of several
43 different spatial parameters, and the incorporation of spectral analysis to describe the texture.

44 Spatial parameters can be obtained in two dimensions (2D) from a linear profile, or in three
45 dimensions (3D) from a surface profile. 2D parameters are predominant in pavement texture
46 characterization since the data collected mainly consist of linear profiles. However, some

1 researchers have recently started to use 3D parameters (17, 18). Spatial texture parameters are
 2 divided into four groups: amplitude, hybrid, spacing, and functional parameters. Amplitude or
 3 height parameters involve the statistical distribution of height values along the Z-axis. Spacing
 4 parameters include the spatial periodicity of the data. The hybrid property is a combination of
 5 amplitude and spacing. The functional parameters give information about the surface structure,
 6 based on the material bearing ratio curve.

7 Table 1 summarizes some of the parameters commonly used for characterization of
 8 pavement texture. The root mean square (RMS) value is used in Mechanical Engineering when a
 9 more accurate measurement of surface texture is required. Some researchers implemented RMS in
 10 highway texture description (9, 10, 17, 19) because it can be used along with the MPD to identify
 11 surfaces with positive or negative texture, which cannot be deduced from measurements of only
 12 MPD or MTD. Additionally, values of Skewness (R_{sk}) and Kurtosis (R_{ku}), offer a good description
 13 of the surfaces regarding the height distribution. Skewness represents the degree of symmetry of
 14 the profile heights about the mean plane. The sign of skewness indicates the predominance of
 15 peaks (positive), or valleys (negative). Kurtosis indicates the presence of extremely high peaks or
 16 depth valleys (higher than 3), or the lack of them (lower than 3). If the profile heights follow a
 17 normal distribution, the value of skewness is 0, and the value of kurtosis is 3.

18 Researchers have also used hybrid parameters to describe pavement surface texture (9, 10).
 19 For instance, the two points slope variance (SV_{2pts}) which measures the slope between two
 20 consecutive points as the difference in height between two consecutive coordinates, divided by the
 21 horizontal distance between them. Also, the six points slope variance (SV_{6pts}), which calculates
 22 the slope using a weighted sum of the height values of six coordinates divided by the horizontal
 23 distance between them.

24
 25 **TABLE 1 Texture Parameters Used for Pavement Texture Characterization**

<i>Amplitude</i>	
Mean Profile Depth (MPD)	$MPD = \frac{1}{2} [\max(h_1, \dots, h_{N/2}) + \max(h_{N/2+1}, \dots, h_N)]$
Height Average (R_a)	$R_a = \frac{1}{N} \sum_{i=1}^N h_i $
Maximum Height (R_z)	$R_z = \max(h_i) - \min(h_i), i = 1..N$
Root Mean Square (RMS)	$RMS = \sqrt{\frac{1}{N} \sum_{i=1}^N h_i^2}$
Skewness (R_{sk})	$R_{sk} = \frac{1}{RMS^3} \sqrt{\frac{1}{N} \sum_{i=1}^N h_i^3}$
Kurtosis (R_{ku})	$R_{ku} = \frac{1}{RMS^4} \sqrt{\frac{1}{N} \sum_{i=1}^N h_i^4}$
<i>Hybrid</i>	
Two Points Slope Variance (SV_{2pts})	$SV_{2pts} = \sqrt{\frac{1}{N} \sum_{i=1}^N \left(\frac{h_{i+1} + h_i}{\Delta x} \right)^2}$
Six Points Slope Variance (SV_{6pts})	$SV_{6pts} = \sqrt{\frac{1}{N} \sum_{i=1}^N \left(\frac{h_{i+3} - 9h_{i+2} + 45h_{i+1} - 45h_{i-1} + 9h_{i-2} - h_{i-3}}{60 \cdot \Delta x} \right)^2}$

26
 27 Where, h_i = height value for coordinate “i”; N = number of coordinates; and Δx = horizontal distance between coordinates

1 METHODOLOGY

2 The methodology section describes the LLS development and data processing and presents the
3 field data collection procedure.

4 LLS Development

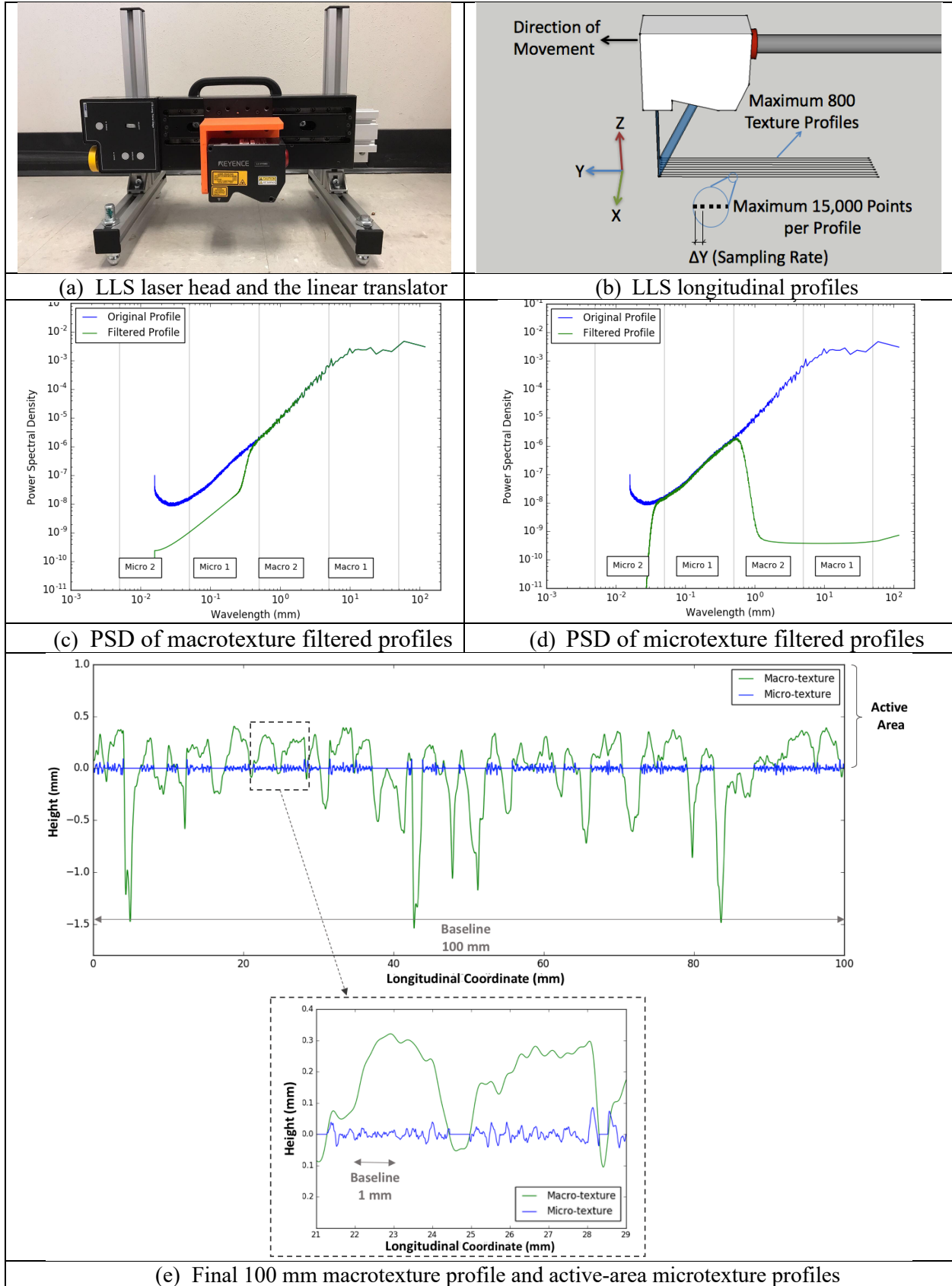
5 As part of this research effort, we implemented a laser scanner equipment (called LLS) to obtain
6 higher-definition of the surface texture. The LLS consists of a line laser head and a linear translator
7 system to control its displacement (*Y-axis*), as shown in Figure 1 (a). Also, we developed a
8 methodological framework to collect texture information using the LLS to characterize both
9 macrotexture and microtexture.

10 The LLS captures the relative-height¹ information of up to 800 profiles in 15 seconds which
11 can be further processed and analyzed to provide a description of the texture. Each profile consists
12 of up to 15,000 data points. The transversal direction is time-independent since the 800 points are
13 captured instantly. The longitudinal direction is time-dependent because the 15,000 points are
14 captured during a period that depends on the laser's sampling frequency. The sampling rate (ΔY)
15 is given by the selected sampling frequency and the linear translator speed. In this study, we used
16 a laser's sampling frequency of 1 kHz and a linear translator speed of 8 mm/s. Thus, the sampling
17 rate is 8 μm , and the total covered area is 120 x 3.26 mm. The analysis is focused on the
18 longitudinal profiles with total length of 120 mm. Figure 1 (b) provides a description of these
19 profiles.

20 The laser repeatability (lower than 2 μm for the *Y-axis*) allows covering the whole
21 macrotexture wavelength range and the first decade of microtexture. In the data processing step,
22 we used Fourier Transform (FT) to convert the signal/data (texture profiles) from the space domain
23 to the texture frequency (or wavelength) domain and to analyze the separate effect of each texture
24 component. The FT transforms the texture profiles into a sum of sinusoidal waves. The output
25 consists of the amplitudes corresponding to each texture frequency. This information can be
26 displayed in a Power Spectral Density (PSD) plot, in which the square of the amplitude is plotted
27 against its corresponding frequency. It can be interpreted as the power or "energy" of a signal (in
28 this case texture) in a specific frequency or wavelength.

29 The relative-height distance obtained by the LLS is transformed to profile height by
30 normalizing with respect to the best-fit line of each profile, a process also known as "detrending."
31 Thus, the profiles are normalized with respect to an average height set equal to zero. After this
32 process, we transform the data to the frequency domain using Discrete FT and then we filter the
33 macrotexture and microtexture information independently using a Butterworth linear filters. The
34 Butterworth filters were designed to be as close as possible to the ideal filter using Python coding
35 language. We used a low-pass filter to isolate macrotexture wavelengths and a band-pass filter to
36 isolate microtexture wavelengths. Figure 1 (c) presents the PSD of the original profile and the low-
37 pass filtered macrotexture, while Figure 1 (d) presents the band-pass filtered microtexture profile.
38 Further details can be found on Zuniga-Garcia (20).

¹ The height information depends on the laser head vertical position. The captured information corresponds to heights relative to the laser head.



1 **FIGURE 1 LLS setup and data processing description**

1 The macrotexture characterization was based on a baseline of 100 mm, while a baseline of
2 1.0 mm was used for microtexture based on findings from previous research (10). We applied the
3 microtexture characterization only to the contact area, which was defined as the tire-pavement
4 interaction area. This contact or “active” area is estimated as the portion of the surface above the
5 mean height of the profiles. Since the profiles were normalized with respect to the average height,
6 the active area corresponds to the positive macrotexture heights. The final profiles obtained are
7 shown in Figure 1 (e). The profiles were then characterized using the different parameters showed
8 in Table 1 for the macrotexture and the microtexture independently. The median value of the
9 parameters obtained for all the baseline-segments was used in the analysis.

10 **Data Collection Procedure**

11 We collected field measurements of friction and texture in the Texas highway network using
12 different tests methods. The friction characterization tests included BPT, DFT, and micro-
13 GripTester, while, the texture characterization tests comprised LLS and CTM. The test sections
14 included a broad range of friction coefficients and texture characteristics. This variety allows a
15 more robust study because it evaluates the relation between texture and friction on different types
16 of pavements and represents the real heterogeneity conditions of a road network. The total number
17 of field samples was twenty-four, including different hot mix asphalt (HMA)² surfaces types aged
18 between 6 to 13 years old: dense-graded Type C (4 samples), Type D (6 samples) and Type F (2
19 samples), porous friction course (PFC) (8 samples), Novachip (2 samples), stone matrix asphalt
20 (SMA) Type C (2 samples).

21 *Sampling Method*

22 The sampling method for the data collection in the field sections consisted of measures of the right
23 wheel path and the center of the outer lane. We collected three different measurements at each
24 section, with a separation of 15 m, as shown in Figure 2 (a). The results reported consisted of the
25 average of the three replicates for the center lane and the right wheel path.

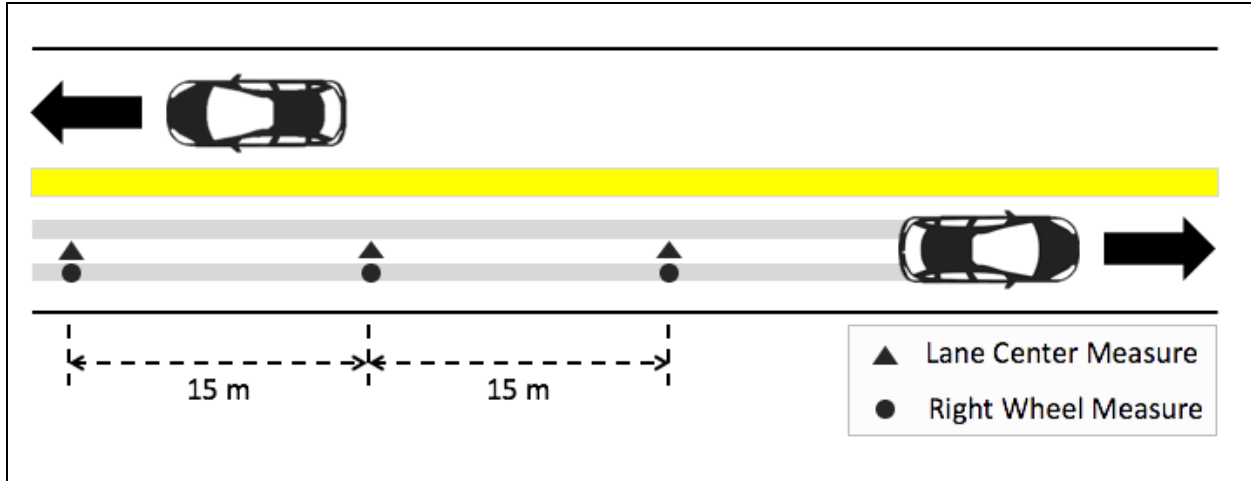
26 *Texture Data Collection*

27 The LLS measurements were made in the same area covered by the CTM. It was located in the
28 sectors A and E of the CTM circumference, corresponding to the traffic direction. The results
29 reported by the LLS consisted of the average of the two measures (sector A and E).

30 *Friction Data Collection*

31 The friction characterization consisted of three different friction tests. The BPT was applied in
32 each of the sampling sites following the traffic direction, as shown in Figure 2 (b). The micro-
33 GripTester, presented in Figure 2 (c), collects a continuous line of frictions measure. The results
34 consist of a series of friction measures, expressed as GN, along the distance evaluated. The GN
35 for each sample was obtained as the average of the GN measures along the total evaluated distance
36 (approximately 30 m). The results obtained from the DFT, shown in Figure 2 (d), are used to
37 estimate the surface friction at different speeds. Two speeds were selected to describe the DFT
38 number (DFTN) at 20 km/h (DFT20), and 60 km/h (DFT60). These parameters were estimated as
39 the average DFTN of the selected speed and a range of values within ± 5 km/h. For instance, DFT20
40 is obtained as the average of DFTN values from a range of speed of 15 to 25 km/h. The use of the
41 average instead of a single value provides a more robust analysis and increases the confidence in
42 the results.

² For details about the HMA specifications refer to TxDOT (21).



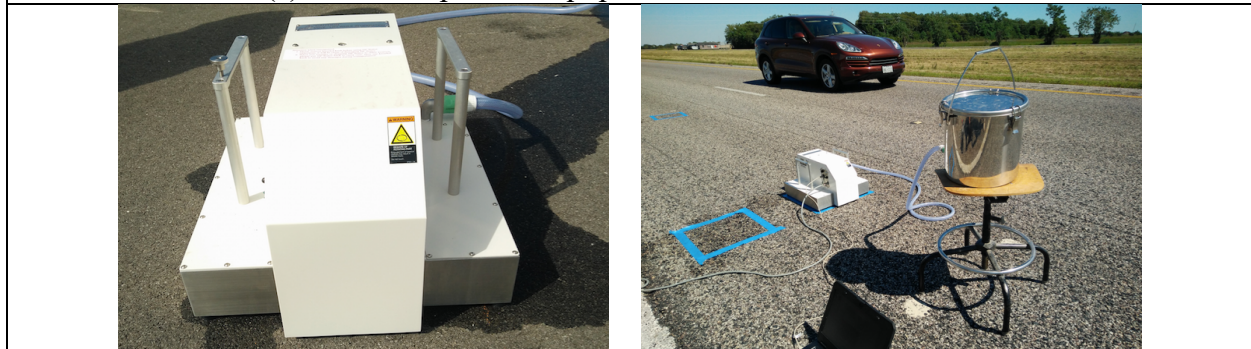
(a) Field test sampling method



(b) British Pendulum Tester (BPT) equipment and field data collection



(c) Micro-GripTester equipment and field data collection



(d) Dynamic Friction Test (DFT) equipment and field data collection

1 **FIGURE 2** Field data collection process

1 STATISTICAL ANALYSIS

2 This section presents the statistical methods used to analyze the collected information with the
3 objective of model friction using macrotexture and microtexture information.

4 Panel Data Analysis

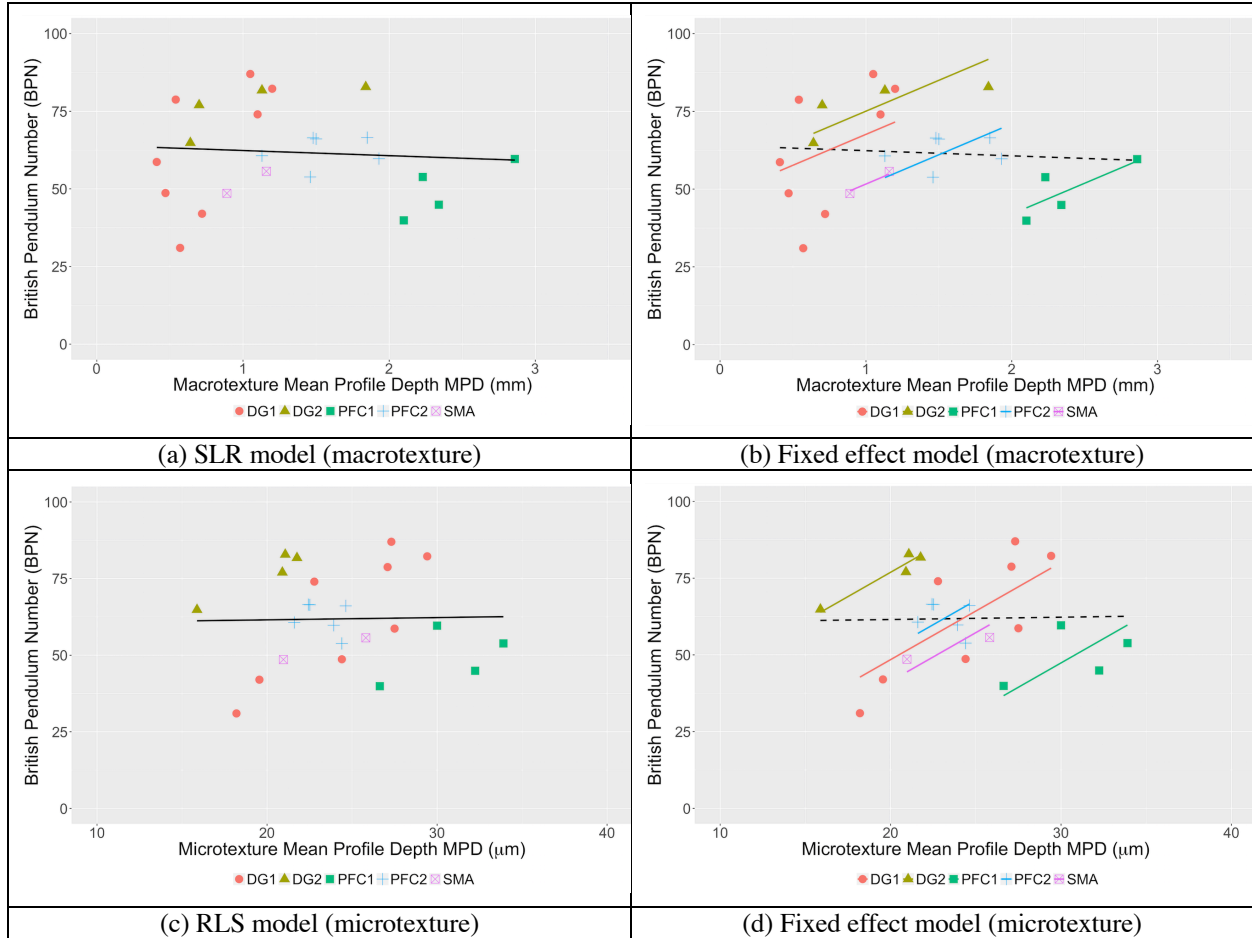
5 From the experimental results, we observed that a simple linear regression (SLR) analysis was not
6 appropriate to model friction because when pooling all the texture data, the correlation between
7 texture and friction was not significant. As an example, Figures 3 (a) and 3 (c) show the friction
8 information obtained from the BPT and the texture represented as MPD value (derived from the
9 LLS) modeled with SLR. We can observe that there is not a significant relationship between the
10 dependent value friction and the independent value, texture. However, the disaggregation of the
11 data by surface type showed a more appropriate relation with positive correlations, as expected
12 based on the theoretical knowledge.

13 Therefore, an SLR analysis cannot be used for the purpose of modeling friction based on the
14 available texture data. A better relation was found when accounting also for the surface type. This
15 fact suggests that it is necessary to include an additional dimension in the analysis. For this reason,
16 a panel data analysis was proposed. A panel data refers to multi-dimensional data including
17 information about multiple phenomena (cross and longitudinal data). The panel data analysis
18 incorporates the use of multiple regression analysis (MRA) and allows the inclusion of the surface
19 type information into the friction model. We use the fixed effect model that considers
20 heterogeneity across surface-type groups and keeps “fixed” (holds constant) the average effect of
21 the texture.

22 We aggregated the samples by surface type and conformed five different HMA homogeneous
23 groups. The first two groups include PFC samples because we divided them into two groups. The
24 PFC pavements tend to present a variety of surface differences depending on the type of asphalt
25 used, age, weather, maintenance, among other factors. The two observed PFC clusters were
26 separated as PFC₁ and PFC₂, since they presented different macrotexture measures, although there
27 is no further information about the characteristics of the surfaces. The first group includes the
28 “coarse” PFC (PFC₁) because its macrotexture was greater than the PFC₂. The second group
29 includes the “fine” PFC sample (PFC₂) and the Novachip mix since it is considered a porous
30 friction course and its macrotexture was similar to the PFC₂ group. The dense-graded mixes were
31 separated into two groups based on the maximum aggregate size. The first group contains the fine
32 mixes Type D and F, and the second group is the coarse mix Type C. The five group are
33 summarized as follow:

- 34 • Type 1 (PFC₁): Porous friction course 1
- 35 • Type 2 (PFC₂): Porous friction course 2 and Novachip
- 36 • Type 3 (DG₁): Dense-graded Type C
- 37 • Type 4 (DG₂): Dense-graded Types D and F
- 38 • Type 5 (SMA): Stone matrix asphalt Type C

39 The proposed analysis includes the use of the fixed effect friction model using texture
40 information and HMA-types. The HMA-types are categorical (or qualitative) variables. Thus, they
41 are incorporated into the models using indicator variables whose possible values are 0 and 1. The
42 variable takes a value of 1 when the sample belongs to the proposed HMA-type, and a value of 0
43 otherwise. Figures 3 (b) and 3 (d) present a comparison of the SLR model (dashed lines) with the
44 fixed effect model. We can observe that we have a constant slope in each case, corresponding to
45 the texture effect, and we have different y-axis intersection values for each HMA group.



1 **FIGURE 3 SLR and fixed effect models for BPN as a function of the MPD.**

2 **Friction Models**

3 We proposed three friction models to evaluate the texture effect on friction measures, presented in
 4 Equations 1 to 3. The Model 1 considers only the macrotexture and HMA-type information for the
 5 independent variables X 's. Therefore, the result of the coefficient β_{Macro} indicates the influence
 6 of the macrotexture over the friction measure, represented by the dependent variable Y_{Fr} . Similarly,
 7 for the Model 2, the β_{Micro} specifies the impact of the microtexture over the friction test. The
 8 Model 3 includes the coefficients for both macrotexture and microtexture. In this case, the model
 9 denotes the effect over the friction measure prediction when incorporating the information of the
 10 two texture components studied. The coefficient values of the indicator HMA-type variables
 11 ($\beta_1, \beta_2, \beta_3$, and β_4) capture the difference between the friction of the evaluated type with respect
 12 to the friction of Type 5 when using a fixed texture parameter value. The β_0 represents the intercept
 13 of Type 5 with the Y -axis, this variable does not have any significant meaning.

14 The three basic models were applied using the four friction measurements obtained from
 15 the tests methods as the dependent variable: BPN, GN, DFT20, and DFT60. Additionally, the
 16 texture measurements include the results obtained from the LLS for both macrotexture (X_{Macro}),
 17 and microtexture (X_{Micro}). The texture information contained in the models corresponds to the
 18 eight parameters obtained from the LLS for each texture component: MPD, RMS, R_a , R_z , R_{sk} , R_{ku} ,
 19 SV_{2pts} , and SV_{6pts} . We estimated the models using the Software R and the combination of variables
 20 give a total of 96 models.

Model 1 (macrotexture only) $Y_{Fr} = \beta_0 + \beta_{Macro}X_{Macro} + \sum_{i=1}^4 \beta_i X_{Type\ i}$ (1)

Model 2 (microtexture only) $Y_{Fr} = \beta_0 + \beta_{Micro}X_{Micro} + \sum_{i=1}^4 \beta_i X_{Type\ i}$ (2)

Model 3 (both macro and micro) $Y_{Fr} = \beta_0 + \beta_{Macro}X_{Macro} + \beta_{Micro}X_{Micro} + \sum_{i=1}^4 \beta_i X_{Type\ i}$ (3)

1 Where,

2 Y_{Fr} = friction measure (BPT, GN, DFT20, or DFT60).

3 X_{Macro} = macrotexture parameter (MPD, RMS, R_a , R_z , R_{sk} , R_{ku} , SV_{2pts} , or SV_{6pts}).

4 X_{Micro} = microtexture parameter (MPD, RMS, R_a , R_z , R_{sk} , R_{ku} , SV_{2pts} , or SV_{6pts}).

5 i = surface type index (Type 1, Type 2, Type 3, or Type 4).

6 $X_{Type\ i}$ = dummy variable equal to 1 if the mixture is Type i and 0 otherwise.

7 Hypothesis Test

8 We used a two-tailed hypothesis test to determine if the independent variables included in the
 9 models (texture and HMA-type) had a statistically significant influence on friction. The confidence
 10 level selected was 95%, i.e., a significance level $\alpha = 0.05$. The null hypothesis (H_0), Equation 4,
 11 establishes that the coefficient (β_i) was equal to 0, meaning that the corresponding independent
 12 variable did not have any impact on the friction. The alternative hypothesis (H_a), Equation 5, states
 13 that the coefficient is distinct from 0, which means that the variable did have a statistically
 14 significant influence on friction. The null hypothesis needs to be rejected to be able to conclude
 15 that the coefficients are different than 0 and that the corresponding independent variable has a
 16 statistically significant influence on the friction with a confidence level of 95%.

17 $H_0: \beta_i = 0$ (4)

18 $H_a: \beta_i \neq 0$ (5)

19

20 Where, i = Macro, Micro, Type 1, Type 2, Type 3, and Type 4.

21 For the hypothesis testing, we analyzed information about the t-static and p-value for each
 22 coefficient value. These two indicators determine whether to reject or not the null hypothesis. The
 23 t-statistic is a ratio of the departure of an estimated parameter from its notional value and its
 24 standard error. The p-value (or observed significance level) represents the probability, assuming
 25 that the null hypothesis is true, of obtaining a value of the t-statistic at least as contradictory to the
 26 null hypothesis as the value calculated from the available sample.

27 We use the p-value to make the final decision of rejecting or not the null hypothesis by
 28 comparing it with the significance level (α), which is the probability of rejecting the null
 29 hypothesis when true (type I error). The p-values must be lower than $\alpha = 0.05$ to reject the null
 30 hypothesis. The SLR models use the coefficient of determination (R^2), as a comparison measure
 31 of which model has a higher correlation between Y and X values, since it measures how close the
 32 data are to the fitted regression line. However, the R^2 is not an appropriate parameter to compare
 33 MRA models, because its value increases every time an additional predictor variable is added to
 34 the model. The coefficient of multiple determination (R_{adj}^2) adjusts the R^2 for the number of
 35 predictor variables in the model. Thus, this indicator is more appropriate to compare models with
 36 a different number of independent variables. For this reason, we obtained the R_{adj}^2 for all the
 37 models analyzed in this study.

1 RESULTS AND DISCUSSION

2 In this section, we present the primary results and provide the discussion that leads to the main
3 findings. We first analyze the friction models including only the MPD as a texture parameter and
4 then evaluate the models that used the other seven parameters.

5 Using the MPD as Texture Parametric Description

6 The MPD is the most widely used macrotexture parameter. For this study, we estimated the
7 macrotexture MPD value using the LLS and compared the results with the CTM, which also
8 provides macrotexture MPD results. The correlation between both values, measured using the
9 correlation coefficient R^2 , is 95% which is considered high. The rest of the analysis includes the
10 MPD based on the LLS only.

11 We estimated the Models 1 to 3 using R software and collected the more relevant
12 information. We modeled friction using the four different friction measures and utilized texture as
13 predictor using the MPD as the parameter for both macrotexture and microtexture. Table 2 shows
14 the results for the t-statistic and p-value for the models' coefficients of interest (β_{Macro} and
15 β_{Micro}), and the R_{adj}^2 for the friction models. The shaded t-statistic and p-values represent the
16 conditions of failing to reject the null hypothesis. Also, Figure 4 presents these results in graphical
17 representation for Models 1 and 2.
18

19 **TABLE 2 Statistical Analysis for the Friction Models Using MPD**

Friction Model	Friction Measure											
	British Pendulum Number (BPN)			Grip Number (GN)			Dynamic Friction Test 20 km/h (DFT20)			Dynamic Friction Test 60 km/h (DFT60)		
	β	t-stat (p-value)	R^2_{adj}	β	t-stat (p-value)	R^2_{adj}	β	t-stat (p-value)	R^2_{adj}	β	t-stat (p-value)	R^2_{adj}
Texture parameter: Mean profile depth (MPD)												
1-Macro only	β_{macro}	2.533 (0.021)	0.357	β_{macro}	1.709 (0.106)*	0.338	β_{macro}	2.602 (0.018)	0.733	β_{macro}	2.786 (0.012)	0.609
2-Micro only	β_{micro}	4.397 (0.000)	0.579	β_{micro}	3.491 (0.003)	0.548	β_{micro}	3.479 (0.003)	0.780	β_{micro}	4.472 (0.000)	0.735
3-Both macro and micro	β_{macro}	2.135 (0.048)	0.649	β_{macro}	1.047 (0.310)*	0.551	β_{macro}	2.136 (0.048)	0.816	β_{macro}	2.487 (0.024)	0.794
	β_{micro}	3.996 (0.001)		β_{micro}	3.008 (0.008)		β_{micro}	3.034 (0.007)		β_{micro}	4.148 (0.000)	

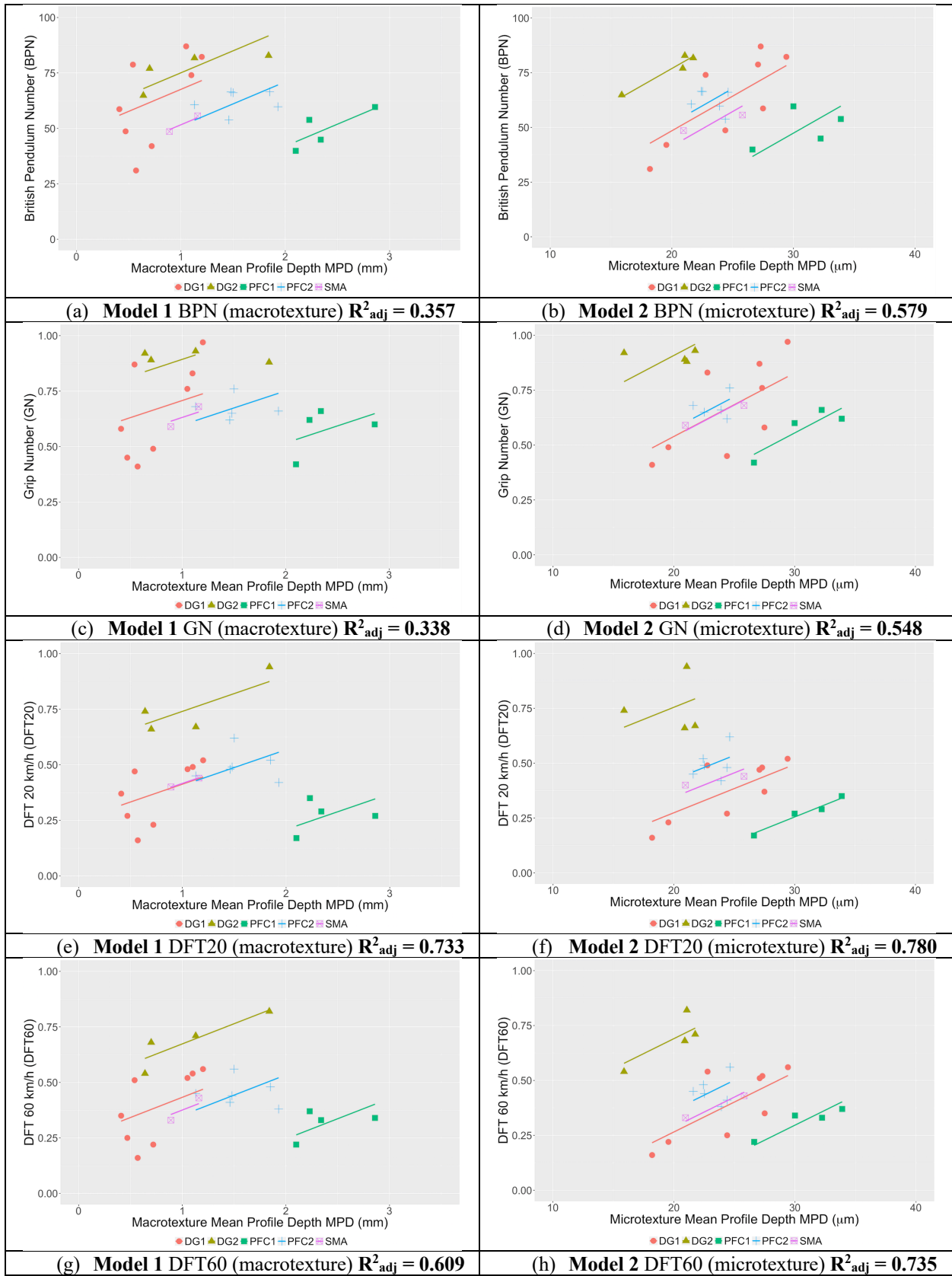
* Note: the shaded t-statistic and p-values represent the conditions of failing to reject the null hypothesis ($|t-stat| < 1.96$ and/or $p-value > 0.05$).

20
21

22 BPT and MPD Parameter

23 Based on the results using BPN as the dependent variable, the Model 1 suggests that the
24 macrotexture has a statistically significant influence on friction. Utilizing the t-statistic and p-
25 value, we can reject the null hypothesis. Similarly, Model 2 indicates that microtexture influences
26 friction. This finding is significant because it proves, with field information, that both macrotexture
27 and microtexture, represented by the MPD, have a statistically significant impact on the friction
28 measured with the BPT. Also, it is important to mention that the R_{adj}^2 is nearly 60% greater for the
29 Model 2 (microtexture) than for the Model 1 (macrotexture). This fact suggests that the
30 microtexture have a more significant impact to the BPT friction than the macrotexture, which is
31 consistent with the theory since at low speeds the microtexture effect is dominant, due to the
32 adhesion mechanism.

33 The results for Model 3 show that both macrotexture and microtexture affect friction and
34 that by including both components into the model, the R_{adj}^2 increased to 0.649, compared to Model
35 1 (0.357) and Model 2 (0.579), where only the individual effects were incorporated. Thus, Model
36 3 is the best model to describe friction obtained by the BPT, using the MPD parameter.
37



1 **FIGURE 4 Friction fixed-effect models using macrotexture MPD and microtexture MPD**

1 *Micro-GripTester and MPD Parameter*

2 The results from MPD and the GN from Table 2 show that using macrotexture information (Model
3 1), the null hypothesis $\beta_{Macro-MPD} = 0$ cannot be rejected. Therefore, the model suggests that the
4 friction cannot be predicted using macrotexture information for the micro-GripTester. However,
5 the Model 2 shows that the microtexture has an effect on GN ($\beta_{Micro-MPD} \neq 0$). Also, the results
6 show that the friction prediction is not improved by incorporating both macrotexture and
7 microtexture information since the Model 3 presents a similar R_{adj}^2 than Model 2, and the
8 $\beta_{Macro-MPD}$ does not have statistical significance. Therefore, the Model 2 is the most appropriate
9 for the micro-GripTester measures. These results can be related to the speed of the test (2.5 km/h).
10 It is apparent that this test is not capturing macrotexture influence due to the low speed.

11 *DFT and MPD Parameter*

12 The DFT allows an evaluation of the relationship texture-friction at a range of speeds. As stated
13 previously, for the present study only two speeds were selected, 20 and 60 km/h. The two cases
14 present t-statistics and p-values that allow the rejection of the null hypothesis, supporting the
15 notion that $\beta_{Macro-MPD} \neq 0$ and $\beta_{Micro-MPD} \neq 0$. Therefore, both macrotexture and microtexture
16 have an influence on the friction obtained from the DFT.

17 The results from the DFT models present values of R_{adj}^2 greater for the Model 2 compared
18 to Model 1, approximately 7% (DFT20) and 19% (DFT60) more. Thus, for all the cases the Model
19 2, which includes only the microtexture, has a better correlation coefficient than Model 1 that only
20 includes the macrotexture. Also, the results show that the Model 3 is the most appropriate model
21 since it presents the higher R_{adj}^2 . The Model 3 includes the information of both macrotexture and
22 microtexture. The greater R_{adj}^2 obtained is 0.816, corresponding to Model 3 when using DFT20 as
23 the dependent variable.

24 **Evaluation of Different Texture Parameters**

25 We evaluated the same models using seven different texture parameters. Table 3 summarizes the
26 results. In this case, we select only the models that performed better for each friction measure. For
27 instance, we show Model 3 for the BPT and the DFT measure and Model 2 for the GN measure.
28 Based on the results, only the R_z parameters have statistical significance for the GN and the DFT
29 measures, similar to the effects observed for the MPD parameter. It is important to mention that
30 the MPD and the R_z were obtained with a similar methodology. Therefore, is likely that these two
31 parameters present comparable results. For instance, the R_{adj}^2 value is similar for the models using
32 these two parameters. However, only the MPD models reject the null hypothesis for both
33 β_{Macro} and β_{Micro} from Model 3 for the BPT measure.

34 The other six parameters do not seem to provide a good correlation with the friction
35 measures. Only the parameters R_a , RMS and SV_2 , and SV_6 offer significant models for the GN
36 values but not for the BPN and DFT values. The results obtained were not expected because the
37 MPD and the R_z measure very simplistic characteristics of the profiles, while parameters such as
38 the SV and R_{sk} provide more details about the height distribution. Thus, we expected a better
39 friction correlation. However, based on the evidence obtained in this study, the MPD appeared to
40 be the better texture characterization parameter to model friction.

1 **TABLE 3 Statistical Analysis for the Friction Models Using Different Texture Parameters**

Friction Measure											
British Pendulum Number (BPN)			Grip Number (GN)			Dynamic Friction Test 20 km/h (DFT20)			Dynamic Friction Test 60 km/h (DFT60)		
Model 3-Both macro & micro			Model 2-Micro only			Model 3-Both macro & micro			Model 3-Both macro & micro		
β	t-stat (p-value)	R^2_{adj}	β	t-stat (p-value)	R^2_{adj}	β	t-stat (p-value)	R^2_{adj}	β	t-stat (p-value)	R^2_{adj}
Texture parameter: Maximum height (Rz)											
β_{macro}	1.906 (0.074)*	0.639	β_{micro}	3.521 (0.003)	0.552	β_{macro}	1.980 (0.064)	0.808	β_{macro}	2.216 (0.041)	0.787
β_{micro}	4.009 (0.001)		β_{micro}			β_{micro}	2.926 (0.009)		β_{micro}	4.153 (0.001)	
Texture parameter: Height average (Ra)											
β_{macro}	1.539 (0.142)*	0.624	β_{micro}	3.665 (0.002)	0.567	β_{macro}	1.434 (0.170)*	0.796	β_{macro}	1.654 (0.117)*	0.768
β_{micro}	4.303 (0.000)		β_{micro}			β_{micro}	3.277 (0.004)		β_{micro}	4.408 (0.000)	
Texture parameter: Root mean square (RMS)											
β_{macro}	1.269 (0.221)*	0.606	β_{micro}	3.656 (0.001)	0.566	β_{macro}	1.284 (0.216)*	0.789	β_{macro}	1.481 (0.157)*	0.759
β_{micro}	4.250 (0.000)		β_{micro}			β_{micro}	3.224 (0.005)		β_{micro}	4.361 (0.000)	
Texture parameter: Skewness (Rsk)											
β_{macro}	3.168 (0.006)	0.433	β_{micro}	0.864 (0.400)*	0.257	β_{macro}	2.623 (0.018)	0.731	β_{macro}	2.642 (0.017)	0.595
β_{micro}	0.534 (0.600)*		β_{micro}			β_{micro}	0.643 (0.529)*		β_{micro}	0.735 (0.473)*	
Texture parameter: Kurtosis (Rku)											
β_{macro}	-4.889 (0.000)	0.622	β_{micro}	0.320 (0.753)*	0.229	β_{macro}	-3.182 (0.005)	0.757	β_{macro}	-3.937 (0.001)	0.699
β_{micro}	-0.093 (0.927)*		β_{micro}			β_{micro}	-0.288 (0.777)*		β_{micro}	0.272 (0.789)*	
Texture parameter: Slope variance 2 points (SV2)											
β_{macro}	-0.048 (0.962)*	0.429	β_{micro}	3.050 (0.007)	0.499	β_{macro}	0.801 (0.434)*	0.779	β_{macro}	0.735 (0.472)*	0.655
β_{micro}	2.499 (0.023)		β_{micro}			β_{micro}	2.151 (0.046)		β_{micro}	2.123 (0.049)	
Texture parameter: Slope variance 6 points (SV6)											
β_{macro}	0.159 (0.875)*	0.458	β_{micro}	3.267 (0.005)	0.524	β_{macro}	1.041 (0.313)*	0.782	β_{macro}	1.057 (0.305)*	0.677
β_{micro}	2.730 (0.014)		β_{micro}			β_{micro}	2.258 (0.037)		β_{micro}	2.341 (0.032)	

* Note: the shaded t-statistic and p-values represent the conditions of failing to reject the null hypothesis ($|t\text{-stat}| < |1.96|$ and/or $p\text{-value} > 0.05$).

2
3

4 **SUMMARY AND CONCLUSIONS**

5 This research study addressed pavement texture characterization and modeled its influence on
6 pavement friction. We developed a 3D laser scanner, called LLS, to measure both macrotexture
7 and microtexture, and provided a description of the data processing techniques used to isolate the
8 profiles. The analysis included empirical data collected around the Texas highway network using
9 different friction devices: BPT, DFT, and micro-GripTester. Furthermore, we used eight different
10 parameters to characterize texture and evaluated friction models using these parameters.

11 Among the major findings, the empirical data suggests that there is not a unique
12 relationship between texture and friction. The relationship between texture and friction is strong,
13 but it is different for each type of surface. Therefore, it is important to include the surface type
14 information when modeling friction. Additionally, we found that models including microtexture
15 present higher correlation and that incorporation both microtexture and macrotexture result in a
16 more appropriate friction estimation. Thus, a measure of microtexture should be included into
17 friction models based on texture. Regarding the texture parametric description, we found that the
18 MPD was the most significant parameter for macrotexture and for microtexture to explain the
19 distinct friction measures.

1 The results and methods proposed in this study can serve multiple purposes. First, from the
2 transportation agencies point of view, the proposed models will allow the accurate estimation of
3 friction using texture data at the network level. As of today, equipment is available to measure
4 macrotexture at highway speed. The research team is currently working on the measurement of
5 microtexture at highway speeds. Once these two types of information are available, the estimation
6 of friction from texture data will be done more efficiently than running friction tests that required
7 frequent stops to refill the water tanks. This contribution would help to manage and monitoring
8 friction information more efficiently. While texture measurements cannot completely replace
9 friction measurements, texture measurements, including macrotexture and microtexture, can safely
10 be used to identify network areas that are potentially having low friction values. Second, we
11 provide empirical evidence of the need for measuring microtexture wavelengths when
12 characterizing pavement surface texture. With the increasing number of researchers acquiring new
13 technology methods to describe the microtexture, there is also a need to provide standard
14 procedures for uniform and comparable characterization techniques. Finally, our results may also
15 have relevance in the field of transportation research. We provide an application of a panel data
16 analysis approach that allows the incorporation of other variables into the models to account for
17 heterogeneity across surface types and provide a more robust analysis.

18 Based on the results of this research study, the research team is currently investigating new
19 hardware both in term of laser technology and data processing technology in an attempt to develop
20 equipment to capture microtexture at highway speed. On the aspect of implementation, the
21 research team is applying the findings of this study to include a wider variety of pavement surfaces
22 and friction measuring techniques. Also, we recommend an evaluation using the Locked Wheel
23 Tester and the GripTester because these devices use higher testing speeds and simulate better real
24 conditions.

25 **Author Contribution Statement**

26 The authors confirm contribution to the paper as follows: study conception and design: Natalia
27 Zuniga-Garcia and Jorge A. Prozzi; data collection: Natalia Zuniga-Garcia; analysis and
28 interpretation of results Natalia Zuniga-Garcia and Jorge A. Prozzi; draft manuscript preparation:
29 Natalia Zuniga-Garcia. All authors reviewed the results and approved the final version of the
30 manuscript.

31 **REFERENCES**

- 32
- 33
- 34 1. Federal Highway Administration (FHWA). (2016). Pavement Friction. Available via:
35 https://safety.fhwa.dot.gov/roadway_dept/pavement_friction/
- 36 2. Rajaei, S., Chatti, K., and Dargazany, R. (2017). A review: Pavement Surface Micro-texture
37 and its contribution to Surface Friction. Transportation Research Board 96th Annual Meeting,
38 Paper 17-06773.
- 39 3. PIARC, (1987). PIARC Technical Committee on Surface Characteristics: Technical
40 Committee Report No 1 to the XVIII World Road Congress, Brussels, Belgium.
- 41 4. Hall, J.W., K.L. Smith, J.C. Wambold, T.J. Yager and Z. Rado (2009). Guide for Pavement
42 Friction. NCHRP Web-Only Document 108. National Cooperative Highway Research Program,
43 Washington, D.C.
- 44 5. Rado, Z., & Kane, M. (2014). An initial attempt to develop an empirical relation between
45 texture and pavement friction using the HHT approach. *Wear*, 309(1-2), 233-246.

- 1 6. Ueckermann, A., Wang, D., Oeser, M., & Steinauer, B. (2015). Calculation of skid resistance
2 from texture measurements. *Journal of traffic and transportation engineering (English edition)*,
3 2(1), 3-16.
- 4 7. Kouchaki, S., Roshani, H., Prozzi, J. A., Garcia, N. Z., & Hernandez, J. B. (2018). Field
5 Investigation of Relationship between Pavement Surface Texture and Friction. *Transportation*
6 *Research Record*, 0361198118777384.
- 7 8. Omar, L. G., Halim, E., Omar, A., & Ismail, K. (2017). Investigating Predictability of
8 Pavement Friction on Rural Roads in Ontario, Canada (No. 17-02502).
- 9 9. Li, S., Noureldin, S., and Zhu, K. (2010). Safety Enhancement of the INDOT Network
10 Pavement Friction Testing Program: Macrotexture and Microtexture Testing Using Laser Sensors.
11 Joint Transportation Research Program FHWA/IN/JTRP-2010/25. Purdue University. West
12 Lafayette, Indiana.
- 13 10. Serigos, P.A., Smit, A., and Prozzi, J. A. (2014). Incorporating Surface Micro-texture in the
14 Prediction of Skid Resistance of Flexible Pavements. In *Transportation Research Record: Journal*
15 *of the Transportation Research Board*, No. 2457, Transportation Research Board of the National
16 Academies, Washington, D.C., pp. 105–113.
- 17 11. Alhasan, A., Smadi, O., Bou-Saab, G., Hernandez, N., & Cochran, E. (2018). Pavement
18 Friction Modeling using Texture Measurements and Pendulum Skid Tester. *Transportation*
19 *Research Record*, 0361198118774165.
- 20 12. American Association of State Highway and Transportation Officials (AASHTO). (2008).
21 AASHTO Guide for Pavement Friction, first ed., Washington DC.
- 22 13. Kogbara, R.B., Masad E.A., Kassem, E. Sparpas A.T. Anupam, K. (2016). A state of art review
23 of parameters influencing measurements and modeling of skid resistance of asphalt pavements.
24 *Construction and Building Materials* 114 602–617.
- 25 14. Henry, J.J. (2000). Evaluation of Pavement Friction Characteristics. NCHRP Synthesis 291.
26 National Cooperative Highway Research Program, Washington, D.C.
- 27 15. Thomas, L. (2008) Grip Tester MK2 D-Type Maintenance Manual. Findaly, Irvine Limited.
28 Midlothian, Scotland.
- 29 16. Masad, E. (2005). Aggregate Imaging System (AIMS): Basics and Applications. Texas: Texas
30 Transportation Institute. FHWA/TX-05/5-1707-01-1.
- 31 17. Madeiros, M.S., Underwood, B.S., Catorena, C., Rupnow, T. Rowls, M. (2016) 3D
32 Measurement of Pavement Macrotexture Using Digital Stereoscopic Vision. *Transportation*
33 *Research Board 95th Annual Meeting*, Paper 16-5504.
- 34 18. Li, Q., Guangwei, Y., Wang, K.C., Zhan, Y, and Wang, C. (2017) Novel Macro- and Micro-
35 Texture Indicators for Pavement Friction Using High-Resolution 3D Surface Data. *Transportation*
36 *Research Board 96th Annual Meeting*, Paper 17-05098.
- 37 19. Gunaratne, M. Bandara, J. Mendzorlan, J. Chawla, M., and Ulrich, P. (2000). Correlation of
38 Tire Wear and Friction to Texture of Concrete Pavements. *J. Mater. Civ. Eng.*,
39 10.1061/(ASCE)0899-1561(2000)12:1(46), 46-54.
- 40 20. Zuniga-Garcia, N. (2017). Predicting Friction with Improved Texture Characterization
41 (Master's Thesis). The University of Texas at Austin, Texas. Available via:
42 <http://hdl.handle.net/2152/47406>
- 43 21. Texas Department of Transportation (TxDOT) (2014). Standard Specifications for
44 Construction and Maintenance of Highways, Streets, and Bridges.